Electric Supplementary Information (ESI)

Electronic Modulation of Iron Phthalocyanine Molecular Catalysts via Cyano-Substitution for Oxygen Reduction Reaction Activity

Kosuke Ishibashi[a], Yutaro Hirai[b,c], Noriko Haiya[d], Tsukasa Ichikawa[d], Nobukatsu Nemoto[d], Yasutaka Matsuo[e], Takayuki Morishima[f], Syeda Anmol Rida[f], Jun Nakamura[f], Shimpei Ono[g], and Hiroshi Yabu[a,b,c*]

Appendix

S1. Materials and methods

S1.1. Materials

KB (EC300J) was purchased from Lion Specialty Chemicals, Co. Ltd., Tokyo. FePc was purchased from TCI, Tokyo, and used without further purification. FePc-8CN and FeAzPc-8CN were synthesized according to the literature. Detail synthetic route and characterizations were shown in the electric supplementary information, S1. dimethyl sulfoxide (DMSO) and 1N KOH aq. were purchased from Fujifilm Wako Chemical Industry, Co. Ltd., Tokyo.

S1.2. Preparation of electrocatalysts

First, 30 mg of KB was dispersed in a dimethyl sulfoxide (DMSO) solution of 0.1 mg/mL of FePc, FeAzPc, FePc-8CN and FeAzPc-8CN. The dispersion was sonicated with a homogenizer for 10 min and then suction-filtered to collect the samples. The samples were washed three times each with methanol and chloroform and then dried in
vacuo.

S1.3. Characterization

XPS was conducted on a JPS9200 spectrometer (JEOL; Al Kα, 10 kV, 10–15 mA). Wide scans were performed from 0 to 1400 eV in 1 eV steps, and narrow scans for each element were performed in 0.1 eV steps. The surface morphologies were observed by using an electron probe micro analyzer (EPMA, JXA-8530F, JEOL, Tokyo, Japan).

S1.4. Electrochemical measurements

ORR performance was evaluated by linear-sweep voltammetry (LSV) measurements using a potentiostat (2325, BAS, Japan). Catalyst inks for each sample were prepared by dispersing 1.0 mg of catalyst in a solution consisting of 7 μL Nafion (527084, Sigma-Aldrich, USA), 430 μL isopropyl alcohol, and 103 μL water by sonication for 10 min. Twenty microliters of the ink was then cast onto the glassy carbon (GC, BAS, Japan) electrode of a rotating ring disk electrode (RRDE, 4 mm diameter, BAS, Japan) and dried. The loading of the catalyst on the electrode was 300 μg/cm^2. A Pt wire and a Hg/HgO electrode were inserted into the electrolyte as counter (CE) and reference electrodes (RE), respectively.

The potential vs Hg/HgO was converted to the reversible hydrogen electrode (RHE) scale using the equation

$$E\ (\text{vs RHE}) = E\ (\text{vs Hg/HgO}) + 0.098 + 0.059\text{V}\cdot\text{pH} \qquad (1)$$

The number of electrons (n) involved in the ORR was calculated from the RRDE results and the following equation:

$$n = \frac{4I_D}{I_D + \frac{I_R}{N}} \quad (2)$$

where I_D and I_R are the current densities of the disk and ring electrodes, respectively, and N is the capture efficiency (0.42).

LSV curves measured in O_2-saturated 1M KOHaq. were calibrated by using a base-line curve measured in N_2-saturated 1M KOHaq.

S1.5. Density functional theory (DFT) calculations

Density function theory (DFT) calculations were carried out using the Gaussian 09 software package with the B3LYP hybrid functional and the 6-311++G(d,p) basis set for C, N, and H and the cc-pVTZ basis set. DFT simulations of the ORR process on catalytic electrodes were performed according to the method based on the computational hydrogen electrode model reported by Nørskov *et al*. Other simulations related to the reaction pathways and free-energy diagrams of the ORR process were performed according to a previously reported method. The adiabatic ionization potential was evaluated as the difference in total energy between the neutral and the +1-charged molecules.

S2. Synthesis of FeAzPc-8CN

Synthetic scheme of FeAzPc-8CN is shown in Figure S1. Detail synthesis methods were shown below.

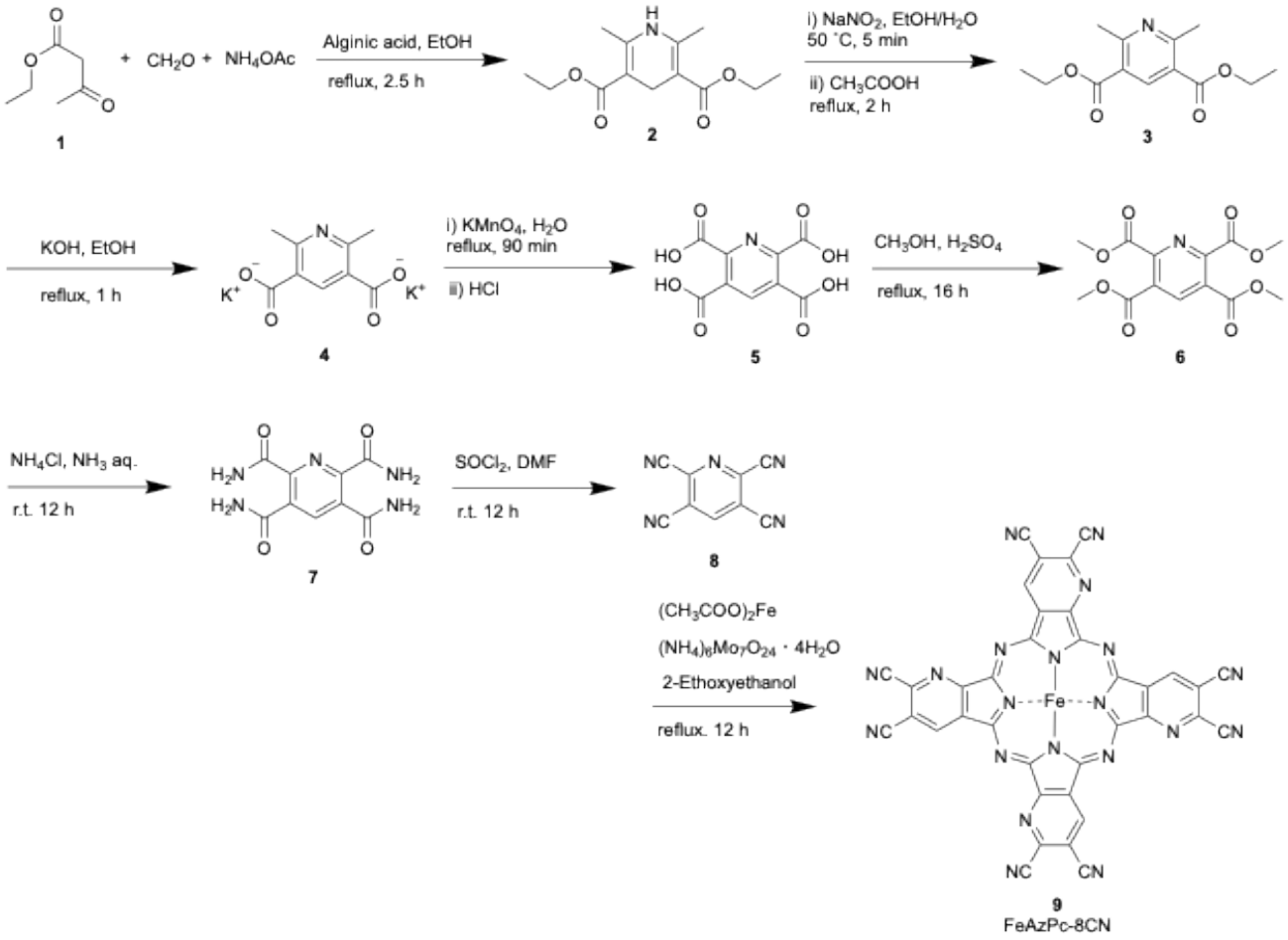

Figure S1. Synthetic scheme of FeAzPc-8N.

S2.1. Materials

Ethyl acetoacetate (Tokyo Chemical Industry Co., Ltd), formaldehyde solution (FUJIFILM Wako Pure Chemical Corporation, Ltd.), ammonium acetate (FUJIFILM Wako Pure Chemical Corporation, Ltd.), alginic acid (NACALAI TESQUE, INC.), sodium nitrite (FUJIFILM Wako Pure Chemical Corporation, Ltd.), acetic acid (KANTO CHEMICAL CO., INC.), potassium hydroxide (KANTO CHEMICAL CO., INC.), potassium permanganate (Tokyo Chemical Industry Co., Ltd), hydrochloric acid (KANTO CHEMICAL CO., INC.), sulfuric acid (KANTO CHEMICAL CO., INC.), ammonium chloride (Wako Pure Chemical Industries, Ltd.), thionyl chloride (KANTO CHEMICAL CO., INC.), urea (Wako Pure Chemical Industries, Ltd.), anhydrous iron(III) chloride (KANTO CHEMICAL CO., INC.), anhydrous cobalt(II) chloride (KANTO CHEMICAL CO., INC.) and pyridine (KANTO

CHEMICAL CO., INC.) were commercially available and used as received. *N,N*-Dimethylformamide (DMF, KANTO CHEMICAL CO., INC.) was used after distillation over calcium hydride. Ethanol (KANTO CHEMICAL CO., INC.) was used after distillation over magnesium and iodine. Diethyl-1,2-dihydro-2,6-dimetylpyridine-3,5-dicarboxylate (**2**), diethyl-2,6-dimethylpyridine-3,5-dicarboxylate (**3**), dipotassium-2,6-dimetylpyridine-3,5-dicarboxylate (**4**), pyridine-2,3,5,6-tetracarboxylic acid (**5**), tetramethylpyridine-2,3,5,6-tetracarboxylate (**6**), pyridine-2,3,5,6-tetracarboxamid (**7**), 2,3,5,6-tetracyanopyridine (**8**), were prepared by the modified methods reported earlier [1-4].

S2.2. Diethyl-1,2-dihydro-2,6-dimetylpyridine-3,5-dicarboxylate (**2**)

Formaldehyde solution (45 mL, 0.600mol), ethyl acetoacetate (**1**, 156.5 g, 1.20 mol), ammonium aetate (55.6 g, 0.721 mol), alginic acid (10.7 g) and ethanol (600 mL) were mixed and the resulting mixture was refluxed for 2.5 h. The reaction mixture was allowed to cool to the ambient temperature and filtered. The resulting solid was dissolved in chloroform and washed with water. The chloroform solution was concentrated under reduced pressure. The residue was recrystallized with the mixed solvent of chloroform and hexane to afford **2** as yellow crystals with the yield of 76 % (116.2 g).

^{1}H NMR ($CDCl_3$, 400 MHz): δ [ppm] 1.29 (t, J = 7.1 Hz, 6H, CH_2-CH_3), 2.19 (s, 6H, NH-C-CH_3), 3.27 (s, 2H, NH-C=C-CH_2), 4.16 (q, J = 7.2 Hz, 4H, CH_2-CH_3), 5.19 (s, 1H, N-*H*).

^{13}C NMR ($CDCl_3$, 100 MHz): δ [ppm] 14.5 (CH_2-*C*H_3), 19.2 (NH-C-*C*H_3), 24.7 (NH-C=C-*C*H_2), 59.7 (*C*H_2-CH_3), 99.5 (N-C=*C*-CH), 144.8 (N-*C*-CH_3), 168.1 (C-*C*OO-CH_2-CH_3).

IR (KBr, cm^{-1}): 1213 (C-O), 1693 (C=O), 2989 (C-H), 3352 (N-H).

T_m: 191 °C.

S2.3. Diethyl-2,6-dimethylpyridine-3,5-dicarboxylate (**3**)

After the mixture of **2** (37.9 g, 0.150 mol), sodium nitrite (20.7 g, 0.300 mol), ethanol (375 mL) and distilled water (150 mL) was stirred at 50 °C for 5 min, acetic acid (18 mL) was added dropwise to this reaction mixture. After the resulting reaction mixture was refluxed for 2 h, it was allowed to cool to the ambient temperature and concentrated under reduced pressure. The resulting solids were washed with water and dried under reduced pressure to afford **3** as white crystals with the yield of 92 % (34.6 g).

^{1}H NMR ($CDCl_3$, 400 MHz): δ [ppm] 1.42 (t, J = 7.1 Hz, 6H, CH_2-CH_3), 2.85 (s, 6H, Ar-CH_3), 4.40 (q, J = 7.2 Hz, 4H, CH_2-CH_3), 8.68 (s, 1H, Ar-*H*).

^{13}C NMR ($CDCl_3$, 100 MHz): δ [ppm] 14.3 (CH_2-*C*H_3), 25.0 (Ar-*C*H_3), 61.4 (*C*H_2-CH_3), 123.0 (N-C-C-*C*H), 140.9 (N-C-*C*-CH), 162.2 (N-*C*-CH_3), 166.0 (C-*C*OO-CH_2-CH_3).

IR (KBr, cm^{-1}): 1223 (C-O), 1718 (C=O), 2977 (C-H).

T_m: 77.1 °C.

S2.4. Dipotassium-2,6-dimetylpyridine-3,5-dicarboxylate (**4**)

Under a dry argon atmosphere, potassium hydroxide (26.4 g, 0.471 mol) in dry ethanol (150mL) was added dropwise to the refluxed solution of **3** (49.0 g, 0.195 mol) in dry ethanol (150 mL). The reaction mixture was refluxed for 1 h and filtered. The collected solids were washed with ethanol and dried to afford **4** as white solids (43.3 g).

^{1}H NMR (DMSO-d_6, 400 MHz): δ [ppm] 2.59 (s, 6H, N-C-CH_3), 8.68 (s, 1H, N-C-C-C*H*).

^{13}C NMR (DMSO-d_6, 100 MHz): δ [ppm] 23.8 (N-C-*C*H$_3$), 133.8 (N-C-C-*C*H), 137.4 (N-C-*C*-CH), 152.9 (N-*C*-C-CH), 171.2 (CH-C-*C*OO$^-$).

IR (KBr, cm^{-1}): 1605 (C=O), 3288 (C-H).

S2.5. Pyridine-2,3,5,6-tetracarboxylic acid (**5**)

Potassium permanganate (71.4 g, 452 mmol) and **4** (15.0 g, 55.2 mmol) in water (500 mL) were refluxed for 90 min. Excess amounts of potassium permanganate was treated with the addition of ethanol. The resulting solution was filtered, and the filtrate was adjusted to pH=1 by adding hydrochloric acid. The mixture was dried under reduced pressure to afford **5** with KCl as white solids (37.4 g).

^{1}H NMR (DMSO-d_6, 400 MHz): δ [ppm] 8.73 (s, 1H, Ar-*H*).

^{13}C NMR (DMSO-d_6, 100 MHz): δ [ppm] 126.5 (N-C-C-*C*H), 153.9 (N-C-*C*-CH), 161.4 (N-*C*-C-CH), 165.2 (CH-C-*C*O-OH), 166.8 (N-C-*C*O-OH).

IR (KBr, cm^{-1}): 1739 (C=O), 3050 (O-H).

S2.6. Tetramethylpyridine-2,3,5,6-tetracarboxylate (**6**)

Sulfuric acid (30 mL) was added dropwise to **5** (28.0 g, mixture with KCl) in methanol (320 mL) at 0 °C, and the reaction mixture was refluxed for 16 h. The reaction mixture was allowed to cool to the ambient temperature and neutralized by sodium bicarbonate solution. The mixture was extracted with ethyl acetate and the organic layer was dried with anhydrous magnesium sulfate and filtered. The filtrate was concentrated under reduced pressure. The resulting solids were recrystallized with the mixed solvent of chloroform and hexane to afford **6** as white crystals with the yield of 6.83 g.

^{1}H NMR ($CDCl_3$, 400 MHz): δ [ppm] 3.99 (s, 6H, CH-C-C-O-CH_3), 4.02 (s, 6H, N-C-C-O-CH_3), 8.75 (s, 1H, Ar-*H*).

^{13}C NMR ($CDCl_3$, 100 MHz): δ [ppm] 53.2 (CH-C-C-O-*C*H$_3$), 53.3 (N-C-C-O- *C*H$_3$), 126,3 (N-C-C-*C*H), 139.8 (N-C-*C*-CH), 152.9 (N-*C*-C-CH), 163.7 (CH-C-*C*O-O-CH$_3$), 165.2 (N-C-*C*O-O- CH$_3$).

IR (KBr, cm^{-1}): 1292 (C-O), 1731 (C=O), 2960 (C-H).

T_m: 117 °C.

S2.7. Pyridine-2,3,5,6-tetracarboxamid (**7**)

After the mixture of **6** (3.00 g, 9.65 mmol), ammonium chloride (0.183 g, 3.34 mmol) and ammonia water (14 mL) was stirred at the ambient temperature for 12 h, it was filtered and washed with water.

The resulting solids were dried under reduced pressure to afford **7** as white crystals with the yield of 86 % (2.07 g).

^{1}H NMR (DMSO-d_6, 400 MHz): δ [ppm] 8.62 (s, 1H, Ar-*H*), 8.63, 7.81, 7.70, 7.48 (s, 8H).

^{13}C NMR (DMSO-d_6, 100 MHz): δ [ppm] 135.6 (N-C-C-*C*H), 136.9 (N-C-*C*-CH), 145.8 (N-*C*-C-CH), 165.1 (CH-C-*C*O- NH_2), 168.8 (N-C-*C*O-NH_2).

IR (KBr, cm^{-1}): 1699 (C=O), 3229 (NH).

T_m: 297 °C.

S2.8. 2,3,5,6-Tetracyanopyridine (**8**)

Under a dry argon atmosphere, thionyl chloride (4.91 g, 41.3 mmol) was slowly added dropwise to **7** (2.20 g, 8.75 mmol) in dry DMF (30 mL) at 0 °C. After the reaction mixture was stirred for 2 h at 0 °C, it was allowed to warm to the ambient temperature and stirred for 12 h. After water was added to quench the excess amount of thionyl chloride, the reaction mixture was extracted with ethyl acetate. The organic layer was dried with anhydrous magnesium sulfate and filtered. The filtrate was concentrated under reduced pressure. The crude product in the residue was purified by silica gel chromatography using the mixed eluent of ethyl acetate/hexane (1:2, v:v). The collected fraction with an R_f value of 0.52 was concentrated under reduced pressure. The residue was recrystallized with ethyl acetate and hexane to afford **8** as white crystals with the yield of 44 % (0.691 g).

^{1}H NMR ($CDCl_3$, 400 MHz): δ [ppm] 8.62 (s, 1H, Ar-*H*).

^{13}C NMR ($CDCl_3$, 100 MHz): δ [ppm] 110.7(N-C-C-*C*H), 111.7(C-*C*-CN), 117.1(N-*C*-CN), 138.7 (CH-C-*C*N), 145.0 (N-C-*C*N).

IR (KBr, cm^{-1}): 2250 (C≡N).

T_m: 209 °C.

References

1. M. G. Dekamin, S. Ilkhanizadeh, Z. Latifidoost, H. Daemi, Z. Karimi, M. Barikani, *RSC Adv.* **4**, 56658 (2014).

2. M. Torabi, M. A. Zolfigol, M. Yarie, B. Notash, S. Azizian, M. Azandaryani, *Sci. Rep.* **11**, 1684 (2021).

3. E. Wöß, U. Monkowius, G. Knör, *Eur. J. Org. Chem*. **19**, 1489 (2012).

4. A. Epstein, B. S. Wildi, *J. Chem. Phys*. **32**, 324-329 (1960).

S2.9. FeAzPc-8CN (**9**)

2,3,5,6-Tetracyanopyridine (0.500 g, 2.79 mmol), Iron(II) acetate (0.121 g, 0.698mmol), DBU (0.1 mL), and ammonium Molybdate tetrahydrate (1 mg) were dissolved in 2-ethoxyethanol (5 mL). The mixture was refluxed for 12h with the oil-bath temperature set to 140 °C. After cooling the reaction mixture to 100 °C, the precipitate was collected by filtration and washed with methanol. The resulting

solid was dried under vacuum at 60 °C to afford as black powder with the yield of 18.5% (98.0mg). Matrix-assisted laser deposition-ionization-time of flight-mass spectroscopy (MALDI-TOF-MS) of the synthesized molecule was performed by using negative mode operation of Autoflex Speed, Bluker Daltonics, US, with using trans-2-[3-(4-tert-butylphenyl)-2-methyl-2-propylidene]malononitrile (Fujifilm Wako Chemical, Japan) as a matrix. The theoretical mass of (**9**) is 772.03 and measured mass peaks are 768.237, 769.237, 770.251, which are attributed to deprotonation compounds of (**9**). Only four hydrogen atoms are present in the pyridine moieties of the molecule. Compound **9** is structurally electron-poor, and therefore, under negative-ion mode conditions, it is reasonable that deprotonation occurs readily at the pyridine ring, resulting in the observed species after loss of a proton. Also, the other smaller molecular weight peaks are attributed to fragments with less CN groups.

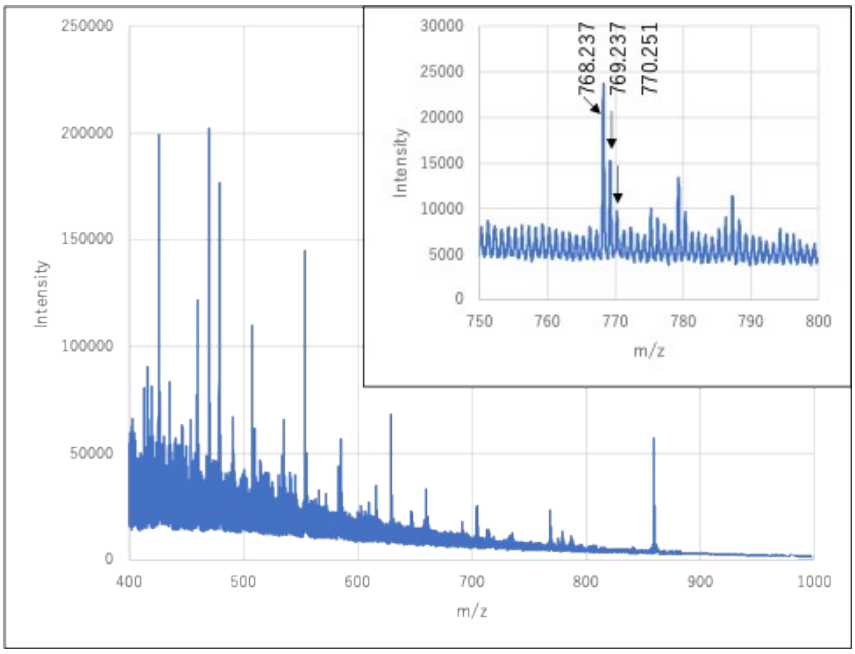

Figure S2. MALDI-TOF-MS spectrum of FeAzPc-8CN (9) (Mw=772.03).

S3. Synthesis of FePc-8CN

Synthetic scheme of FeAz-8CN is shown in Figure S2. Detail synthesis methods were shown below.

2,3,5,6-Tetracyanopyridine (0.500 g, 2.79 mmol), Iron(II) chloride tetrahydrate (0.139 g, 0.702mmol), DBU (0.1 mL), and ammonium Molybdate tetrahydrate (1 mg) were dissolved in 2-ethoxyethanol (20 mL). The mixture was refluxed for 12h with the oil-bath temperature set to 140 °C. After cooling the reaction mixture to 100 °C, the precipitate was collected by filtration and washed with methanol. The resulting solid was dried under vacuum at 60 °C to afford as black powder with the yield of 60.1% (324mg). MALDI-TOF-MS of the synthesized molecule was performed by using negative mode of Autoflex Speed, Bluker Daltonics, US, with using trans-2-[3-(4-tert-butylphenyl)-2-methyl-2-propylidene]malononitrile (Fujifilm Wako Chemical, Japan) as a matrix.

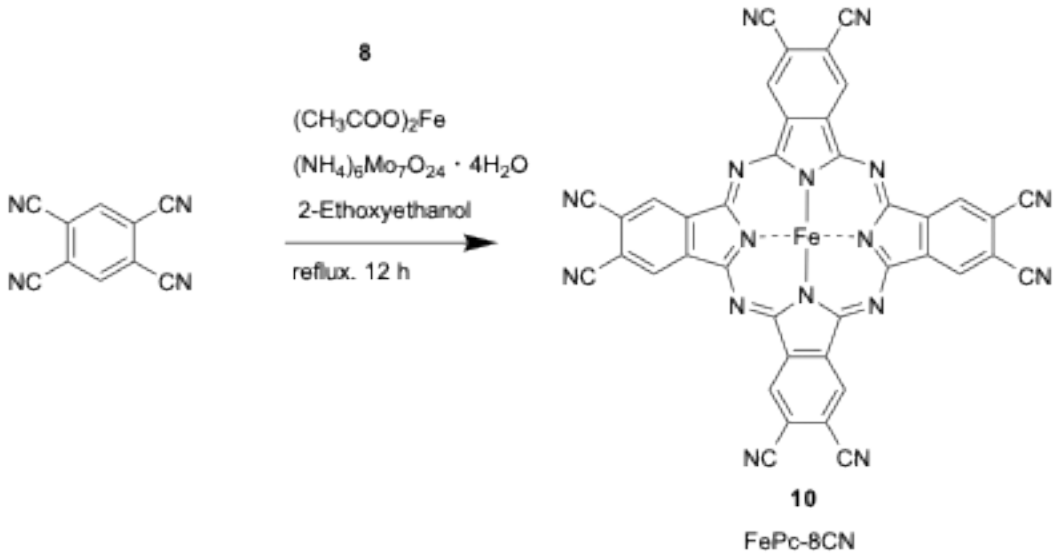

Figure S3. Synthetic scheme of FeAz-8CN (**10**).

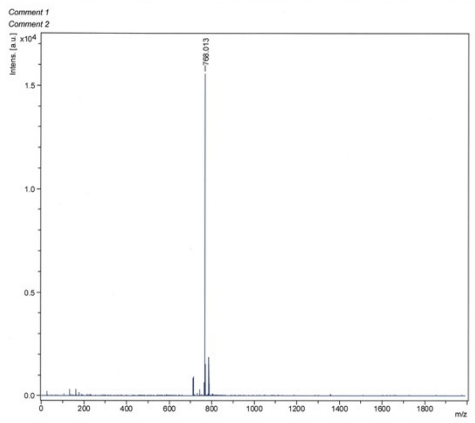

Figure S4. MALDI-TOF-MS spectrum of FeAz-8CN (**10**) (Mw=768.46).

S4. EXAFS analysis

Detail EXAFS analysis parameters and obtained parameters from respective catalysts are shown in Table S1 and S2, respectively.

Table S1. Fitting parameters of EXAFS spectra.

Parameter	Setting
S_0^2	0.8 fixed
N	4 fixed
k-range	3–9 $Å^{-1}$
k-weight	3
R-range	1.0–2.1 Å
Fit parameters	ΔE_0, ΔR, σ^2
Model	FePc-derived Fe–N first-shell path

Table S2. Obtained parameters from EXAFS analysis.

Sample	ΔE_0 / eV	ΔR / Å	σ^2 / $Å^2$	Reff / Å	Fe–N distance / Å	R-factor
FeAzPc-4N	1.358	0.06659	0.00642	1.92520	**1.99179**	0.07538
FePc	2.490	0.01082	0.00481	1.92520	**1.93602**	0.03658
FeAzPc-4N-8CN	0.981	0.08006	0.00588	1.92520	**2.00526**	0.06932
FePc-8CN	-0.096	0.02532	0.00322	1.92520	**1.95052**	0.03521

S5. Relationship between rate limiting steps and Tafel slope values

The Tafel slope values correspond to the following rate-determining steps.

O_2 + H+/e- + * ⇌ OOH*	(120 mV/dec)	(1)
OOH* + * ⇌ O* +OH*	(60 mV/dec)	(2)
O* + H+/e- ⇌ OH*	(24 mV/dec)	(3)
2(OH* + H+/e- ⇌ H_2O + *)	(40 mV/dec)	(4)

Based on these values, steps (3) and (4) are considered to be the dominant rate-determining steps (Fig. 4(c)).

S6. UPS results

Figure S3 shows UPS spectra of FePc-8CN and FeAzPc-8CN at their powder state or on KB. UPS spectra of the catalysts were recorded by using a photoelectron spectrometer (AC-3, RIKEN KEIKI, Japan). Catalyst samples were ground using a mortar and pestle to prepare homogeneous powders. An Al sample stage was filled with a catalyst powder sample, and its UPS spectrum was acquired under normal atmosphere with an irradiation light intensity of 70 nW and an irradiation time of 20 s. The spectra were recorded from 4.00 to 7.00 eV, and the measurement step was 0.100 eV. Ionization potentials (IPs) of the respective catalysts were estimated from the inflection point of their UPS spectrum.

IP values of FePc and FeAzPc shown in the Table 1 are derived from the previous literature[14].

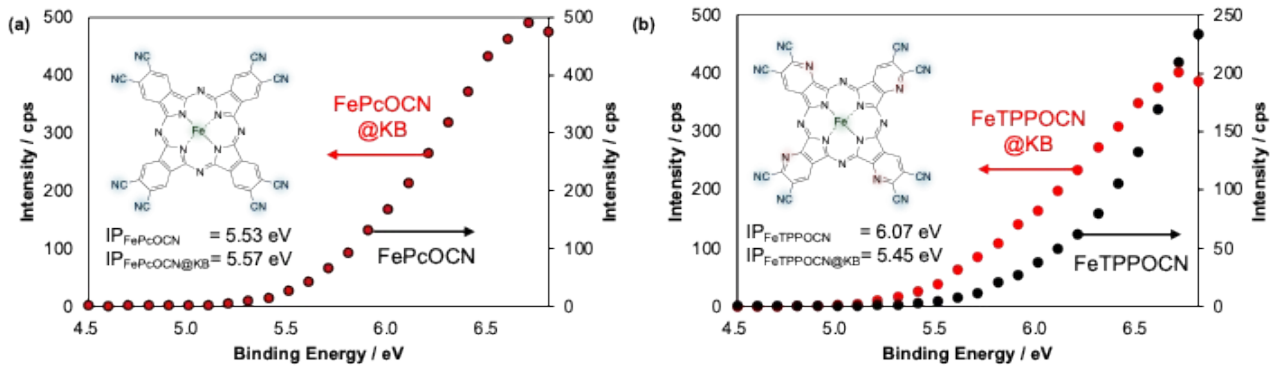

Figure S5. UPS spectra of FePc-8CN (a) and FeAzPc-8CN (b) at their powder state (black) or on KB (red), respectively.

S7. Koutecký–Levich plot

Koutecký–Levich (K-L) plot at 0.2 V vs RHE of each catalyst was obtained from LSV curves obtained by RRDE measurement with changing rotating speed from 400 rpm to 3,600 rpm (Figure S6).

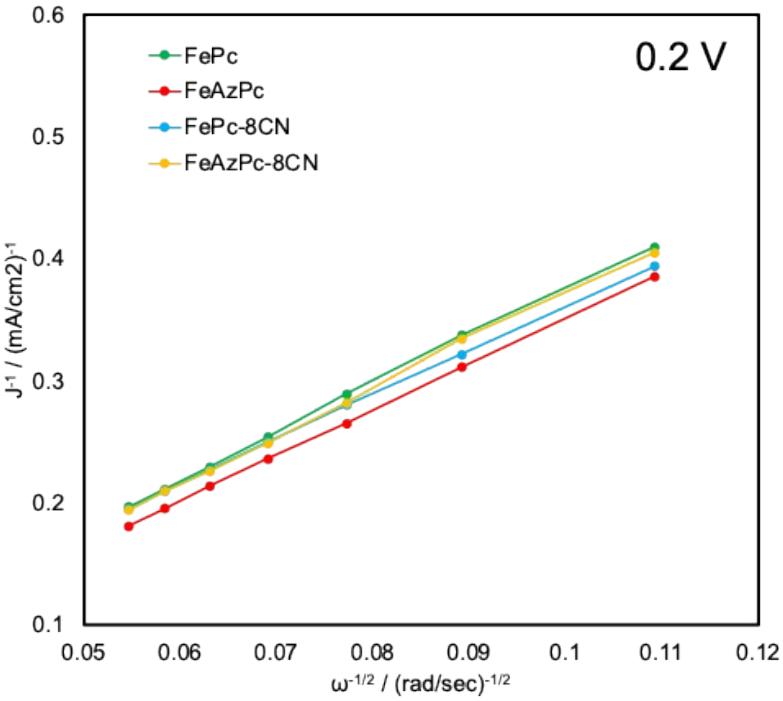

Figure S6. K-L plot of FePc@KB (green), FeAzPc@KB (red), FePc-8CN (light blue), FeAzPc-8CN (yellow), respectively.

The number of electrons (n) involved in the ORR was calculated according to the K–L equation:

$$\frac{1}{J}=\frac{1}{J_k}+\frac{1}{J_d}=\frac{1}{nFAkC_{O_2}}+\frac{1}{0.62nFAD_{O_2}^{2/3}\nu^{-1/6}C_{O_2}\omega^{1/2}}, \qquad \text{(S1)}$$

$$J_k = (J * J_d)/(J_d - J) \qquad \text{(S2)}$$

where J, J_k, and J_d are the measured, kinetic, and diffusion-limited current, respectively; F is the Faraday constant (96,485 C/mol); A is the electrode area (0.1256 cm^2); k is the rate constant for oxygen reduction (M/s); D_{O2} is the diffusion coefficient of O_2 in the electrolyte (1.8×10^{-5} cm^2/s); v is the viscosity of the electrolyte solution (0.01 cm^2/s); C_{O2} is the saturated concentration of O_2 in the electrolyte (7.8×10^{-7} mol/cm); and ω is the angular rotation rate[5]. From the K-L plot, n values of FePc@KB, FeAzPc@KB, FePc-8CN, FeAzPc-8CN were 3.32, 3.91, 3.91, 3.23, respectively

[5] J. Quo, et al., *Inter. J. Electrochem. Sci.*, **8**(1), 1189 (2013).

S8. ECSA

Cyclic voltammogram (CV) of catalysts were measured by using RRDE. Figure S shows CV curves obtained with changing scanning rates.

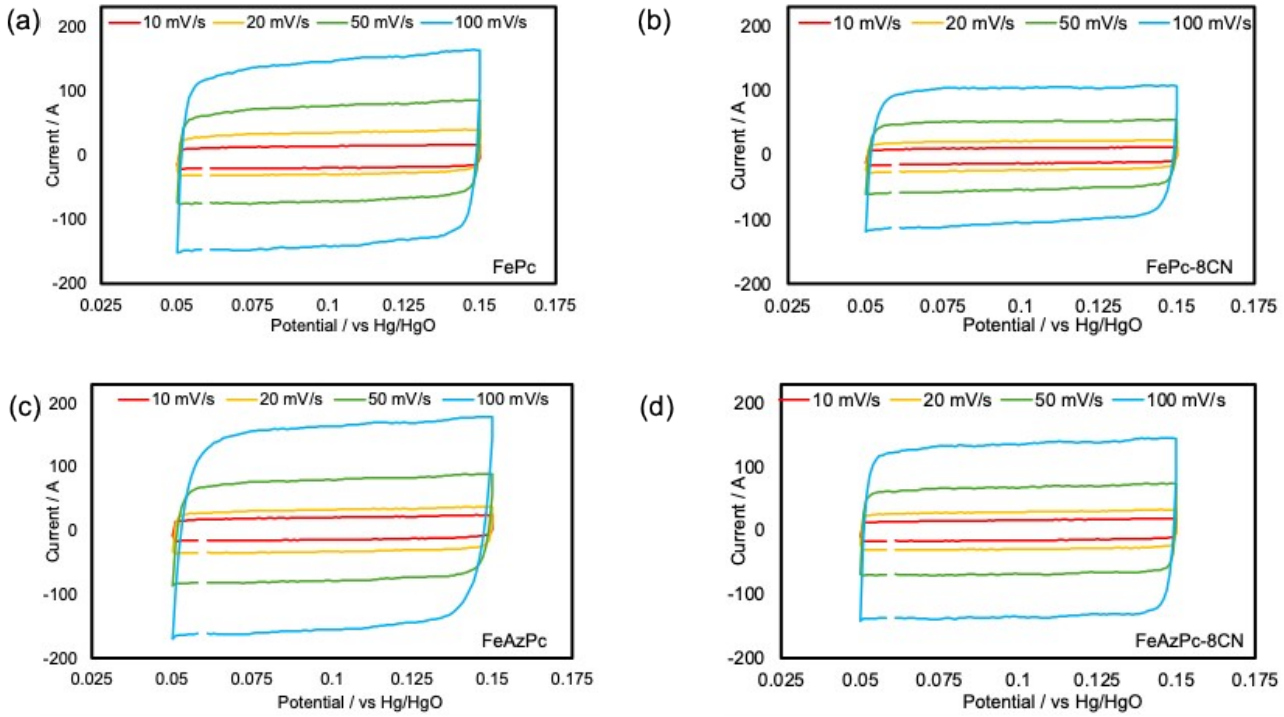

Figure S7. CV curves of catalysts (a) FePc@KB, (b) FePc-8CN@KB, (c) FeAzPc@KB, (d) FeAzPc-8CN@KB, obtained with changing scanning rates from 10 mV/s to 100 mV/s.

From the CV curves, plots of scan rates and current density were prepared (Figure S.).

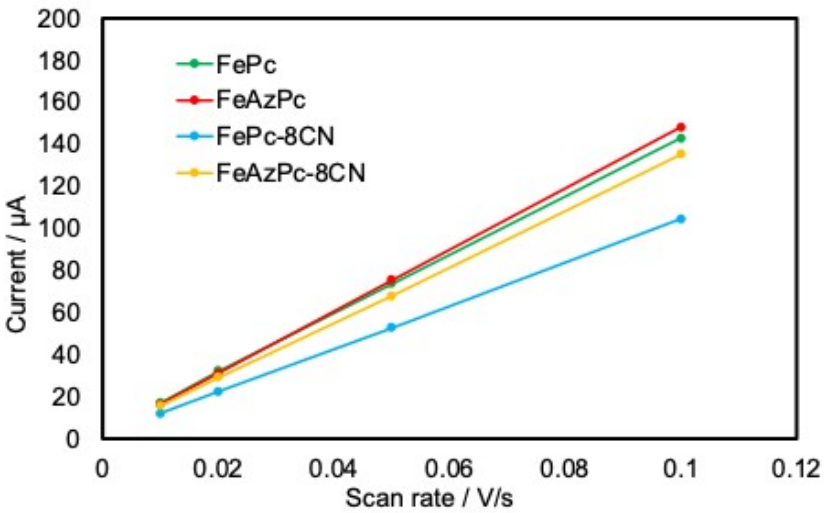

Figure S8. Plots of current density in terms of scanning rates.

ECSA was calculated by

$$ECSA = \frac{C_{dl}}{C_s} \quad (1)$$

where, C_{dl} and C_s were the capacitance of electric double layers and specific capacitance (0.04 mF/ cm^2). C_{dl} was estimated from the double-layer charging current (Dj) and scan rates.

$$C_{dl} = \frac{Q}{V} = \frac{\Delta J \cdot s}{V} = \frac{\Delta j}{V/s} \quad (2)$$

From this equation, the C_{dl} values can be estimated by the slope of the plot in Figure S1(c) and S1(d). Table S3 shows calculated values of ECSA and related parameters.

Table S3. ECSA and related parameters.

	Cdl / µF	ECSA / cm^2	ECSA(g) / m^2/g	RF / cm^2/cm^2
FePc	1,395	34.9	115.5	278
FeAzPc	1,469	36.7	121.6	292
FePc-8CN	1,029	25.7	85.2	205
FeAzPc-8CN	1,326	33.2	109.8	264

S9. Comparison with other catalysts

Table S4. Comparison of ORR activities of metal-phthalocyanine catalysts reported in recent papers.

Catalyst	E_{onset} [V vs RHE]	$E_{1/2}$ [V vs RHE]	Reference
FePc/rGO	0.97	0.86	*RSC Adv.*, 11, 15927-15932 (2021).
FePc@SN950	0.97	0.92	*Sustainable Energy Fuels*, 8, 4344-4354, (2024).
FeCoPPc-ClO_3	0.986	0.923	*Chem. Eng. J.*, 499, 156609 (2024).
FePc@B-RGO	0.95	0.85	*Mol. Cat.*, 587, 115500 (2025).
FePc@CNF	0.966	0.875	*J. Colloid Interf. Sci.*, 562, 213-223 (2020).
FeNiPc/MWCNT	0.94	0.87	*ChemElectroChem*, 9(20), e202200717 (2022).
FeNiPc/G	0.94	0.86	*ACS Appl. Energy Mater.* 2(9), 6634–6641 (2019).
FePc@KB	0.957	0.917	*This work*
FeAzPc@KB	0.985	0.942	*This work*
FePc-8CN@KB	0.972	0.930	*This work*
FeAzPc-8CN@KB	0.944	0.887	*This work*